Pergamon

Journal of Structural Geology, Vol. 16, No. 8, pp. 1129 to 1138, 1994

0191-8141/94 $07.00+0.00

0191-8141(93)E0012-A

Orthorhombically arranged vein arrays

DAVID L. KIRSCHNER and CHRISTIAN TEYSSIER

Department of Geology and Geophysics, University of Minnesota, Minneapolis, MN 55455, U.S.A.

(*Received* 19 *February* 1993; *accepted in revised form* 8 *November* 1993)

Abstract—It is commonly accepted that arrays of en échelon veins occur either singularly or in conjugate pairs. Bulk finite plane strain is accompanied by these singular or conjugately arranged arrays when their formation and subsequent displacement occur in the same kinematic framework. A new geometric and kinematic model for vein arrays is proposed which takes into account the effects of bulk non-plane-strain deformations on the evolving arrays. In this model, four sets of arrays develop during coaxial non-plane-strain deformations and two non-conjugate sets of arrays develop during non-coaxial non-plane-strain deformations. The formation of singular and conjugate arrays is restricted to bulk plane-strain deformations. This model is the natural extension to the brittle–ductile realm of models proposed for the geometry and kinematics of brittle faults formed during non-plane-strain deformations. En échelon vein arrays mapped in central Australia which cannot be understood as simple conjugate structures, are interpreted as having formed during a bulk non-coaxial non-plane-strain deformation.

INTRODUCTION

IT IS commonly accepted that arrays of en échelon veins occur either singularly or in conjugate pairs. In this paper we document contemporaneous en échelon vein arrays that do not display the geometry, symmetry and kinematics of conjugate structures. In order to explain the formation of these arrays we propose another model in which up to four sets of orthorhombically arranged arrays can develop depending on the imposed bulk strain (Fig. 1). In this model conjugate arrays form during bulk coaxial plane strain, while four sets of orthorhombically arranged arrays form during bulk coaxial, non-plane strain. During non-coaxial deformation, the number of arrays are reduced to one for plane strain and two for non-plane-strain deformation. If this model is correct, then it can no longer be assumed that en échelon vein arrays form only singular or conjugate pairs for such geometries are particular only to plane strain conditions.

The central Australian vein system documented in this study shows a high degree of symmetry with fold elements and fracture sets, consistent with the folds, fractures and veins developing under the same, non-plane strain kinematic conditions. First we document the geometry and symmetry of these structures, and discuss their relationships to bulk deformation. Then, we present our model for the formation of en échelon vein arrays, and briefly discuss similar models proposed by Oertel (1965), Aydin (1977), Reches (1978a,b, 1983) and Krantz (1988, 1989) to explain the geometry and kinematics of brittle faulting, since our ideas have been strongly influenced by and are the natural extension of their models from the brittle to the brittle–ductile realm.

STRUCTURAL ASSOCIATIONS AT WHITE RANGE

The veins of this study are located within the 25 km^2 White Range duplex (Fig. 2) (Kirschner & Teyssier

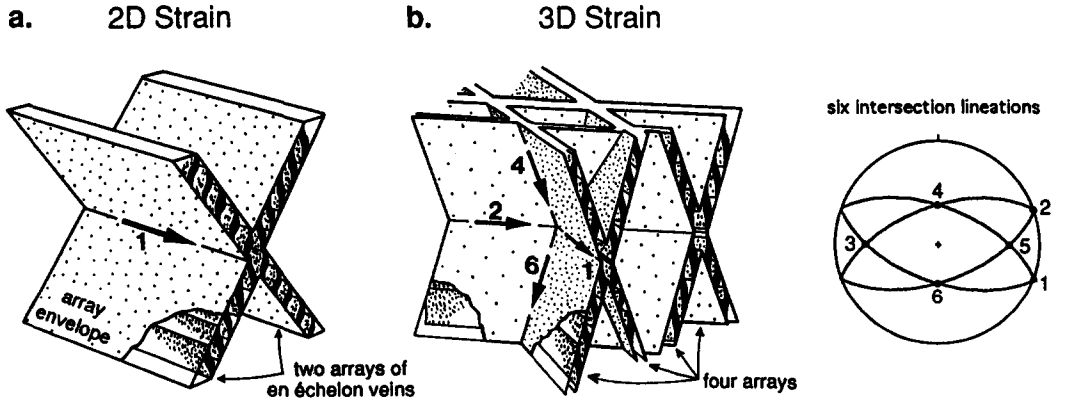

Fig. 1. (a) Conjugate arrays of en échelon veins develop during coaxial plane strain (reproduced with minor changes from Wilson 1982 and Ramsay & Huber 1987). (b) Proposed orthorhombic arrangement of arrays of en échelon veins which develop during bulk triaxial deformations. Contrary to the one intersection lineation in conjugate arrays, orthorhombically arranged arrays have six intersection lineations between vein arrays.

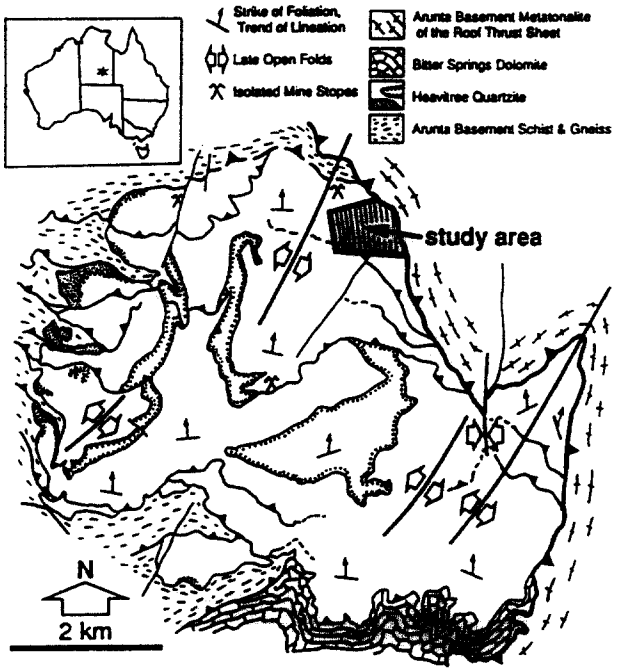

Fig. 2. A vein system composed of orthorhombically arranged arrays is located on the exposed northeast margin of the White Range duplex, central Australia. The gold–sulphide–quartz vein system, which overprints all of the duplex-related structures, is localized along the quartzite–basement thrust contact near the hinge zone of a large, late NE-trending antiform. The vein system was mined circa 1900–1910 and 1989–1991.

1992), which is a stack of isoclinally folded nappes of Late Proterozoic Heavitree Quartzite structurally overlain by a regional thrust sheet composed of Early Proterozoic basement gneisses. The ductile duplex developed during crustal-scale, north-over-south thrusting associated with the Devonian to Carboniferous Alice Springs Orogeny (Forman 1971, Shaw *et al.* 1971, Stewart 1971, Collins & Teyssier 1989, Dunlap *et al.* 1991, Dunlap 1992). The duplex-related structures (foliation, lineation, ductile thrust zones, isoclinal folds) are overprinted by NE-trending open folds and faults, multiple fracture sets and a gold-bearing vein system particularly well developed along the exposed northeastern margin of the duplex. Both the duplex-related structures and the late folds, faults, and veins are interpreted as having developed progressively during the Alice Springs orogeny.

Gold-bearing quartz veins developed within the Heavitree Quartzite along the northeastern margin of the White Range; these veins are the focus of this study. The undeformed to moderately deformed gold-bearing quartz veins microscopically exhibit undulatory extinction, optical subgrains and deformation bands, a few recrystallized grains, and ubiquitous secondary fluid inclusion planes. These mineralized veins, which are localized almost exclusively on the eastern limb of the large antiform, do not extend upward into the basement gneisses.

Gold mining at the turn of the century resulted in the formation of hundreds of small S-dipping mine stopes cutting downwards through the quartzite (Mackie 1986). Recent open pit mining (1989–1991) in the same area has drastically modified the land surface and provided excellent exposure of the veins.

Folds

The large-scale outcrop pattern of the White Range is controlled by a series of NE-trending, open, upright folds (Figs. 2 and 3a). Foliation orientations were recorded throughout the Range in order to constrain the mean orientation of the fold elements. The best-fit fold axis is ~012, 17°N (trend and plunge): the great circle defining the mean fold axis, however, is not well constrained (Fig. 3a) and some crenulations associated with the large open folds trend more easterly (Kirschner & Teyssier 1992). The gold-bearing vein system is situated on the eastern limb of the largest antiform (Fig. 2), and the rest of the paper focuses on this area.

Small late S-verging folds of the mylonitic quartzite fabric with subhorizontal E–W-oriented hinges are localized underneath the basement thrust contact and are proximally associated with the veins and arrays. Most of these small folds are associated with the growth and rotation of individual sigmoid veins. Some minor folds are not associated with veins but developed during minor residual movement of the overlying thrust sheet.

Fractures

The Heavitree Quartzite, along the broad hinge zone of the large antiform, contains a number of fracture sets. The fractures are predominantly smooth, subplanar and continuous for meters to tens of meters. Apart from a few fractures exhibiting weakly developed plumose structures and fringe fractures, surface morphologies commonly associated with extensional fractures (Pollard & Aydin 1988) were not observed. Adjacent coplanar fractures are spaced up to a few meters apart. Since no consistent crosscutting relations between fracture sets were observed, all of the fractures are interpreted to have formed more or less synchronously. The fracture system is one of the last, if not the last, structure to have formed in the White Range.

Fracture orientations were measured along the eastern limb and hinge zone of the large antiform. Care was taken to measure fractures on all available open pit and stope walls in order to representatively capture all the fracture sets and minimize any bias in the data. Few measurements of fracture orientations were recorded along the western limb of the same antiform.

Five moderately distinct steeply dipping sets (sets A–E) are defined by concentration maxima in the contoured fracture data (Fig. 3b). Two sets (A and B) with a dihedral angle of approximately 47° might be grouped together as one conjugate pair. Fracture sets C and E can also be grouped as one conjugate pair with a dihedral angle of approximately 54°. Fracture set D bisects the conjugate fracture sets C and E. Regardless of how the fractures are interpreted, it is important to note that the plane of symmetry that acutely bisects the A–B pair intersects the representative great circles of fracture sets

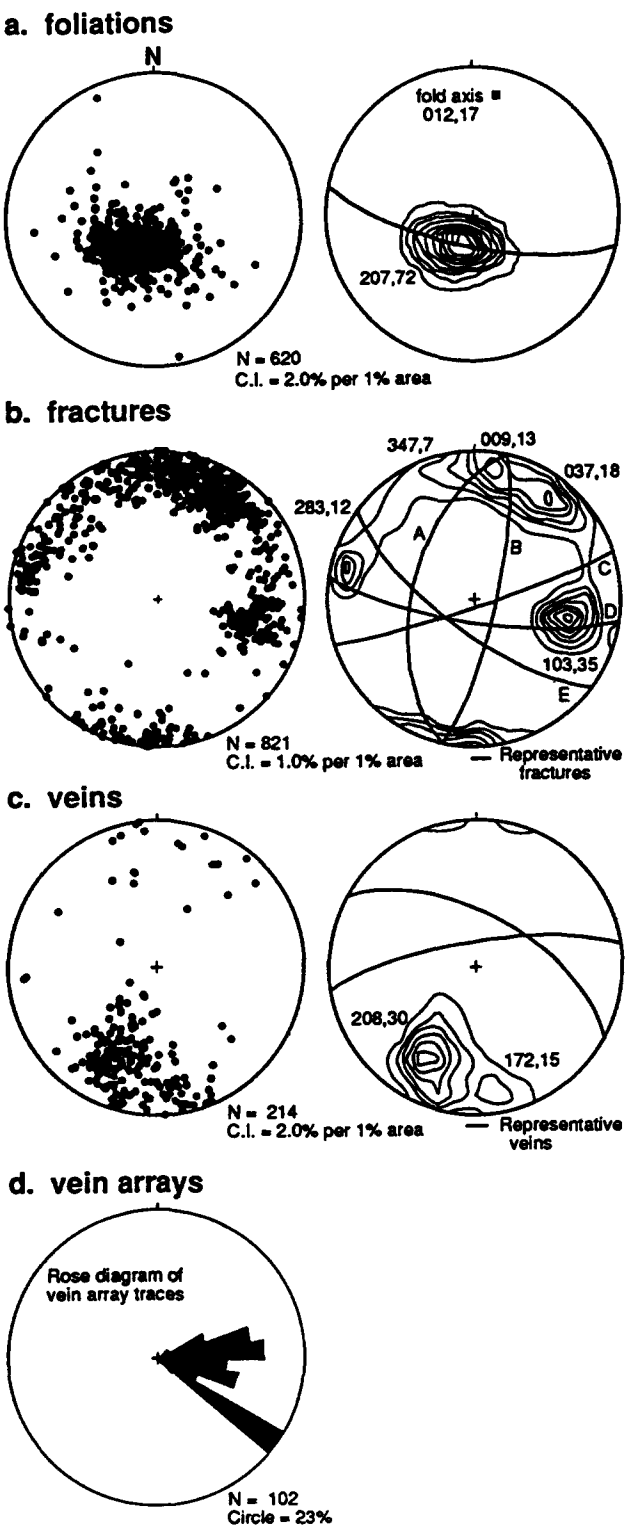

Fig. 3. (a) Foliation formed during the development of duplex is folded about a NE-trending fold axis to form open, upright anitforms and synforms. (b) Fracture sets A–E cross-cut the duplex-related structures and exhibit orthorhombic symmetry. (c) Individual quartz veins in en échelon vein arrays dip toward the south. (d) Rose diagram of vein array traces show two populations, one trending ENE and the other ESE. (Diagrams a, b, and c are Schmidt lower-hemisphere stereonets; C.I. stands for contour intervals.)

C, D and E along *one* line (approximately 235,71°S, trend and plunge). This singularity of intersection supports the hypothesis that all the fractures formed synchronously.

Veins and vein arrays

The following terminology will be used to describe the geometry of the veins. Planar or sigmoid veins aligned en échelon form a vein array or en échelon vein array. A vein array in proximity with other coplanar arrays form a set of arrays. Two sets of arrays which are conjugately arranged form a conjugate pair. All of the spatially and temporally related veins, arrays and sets in the area form a vein system.

The vein system in the White Range is characterized by N-dipping planar or sigmoid veins forming S-dipping en échelon vein arrays (Figs. 3c and 4a&b). Individual veins are centimeters to meters wide, and up to tens of meters long. Though some isolated veins are planar, most veins are sigmoid with thin vein tips that dip steeply to the north (on average 80°N), and thick central portions more shallowly dipping to the north. The fold (rotation) axes of individual sigmoid veins trend approximately E–W and are subhorizontal. Rare S-dipping individual veins are much smaller in size and either are isolated or bifurcate from N-dipping veins. The planar mylonitic foliation in the quartzite is either truncated by the veins along a sharp angular discontinuity, or more commonly, folded about an E–W axis at the vein contact. This folding of the mylonitic fabric resulted from the sigmoid development of the individual veins. A mineral lineation located along the vein–quartzite contacts lies in a subvertical plane. The orientations of these folds and mineral lineation are consistent with the principal plane of movement approximately oriented N–S and subvertical.

Individual N-dipping veins are arranged into S-dipping en échelon arrays which are typically 5–10 m high (Figs. 4a&b). The central zones of these arrays are composed almost entirely of vein material separated by thin 'enclaves' of Heavitree Quartzite. The widths of the S-dipping arrays are generally on the order of several meters. The angle between the steeply inclined N-dipping vein tips and the imaginary envelopes of the moderately inclined S-dipping arrays averages 30–40° (Fig. 4b). The line of intersection between individual veins and the imaginary envelope of the en échelon array is oriented approximately E–W and subhorizontal. Visual observations and drill-hole data suggest the majority of en échelon arrays dip 60–80° to the south. No N-dipping en échelon arrays were observed.

These 5-10 m high S-dipping en échelon arrays are in turn arranged en échelon into larger S-dipping zones (Fig. 4c). The vertical extent of these large en échelon zones cannot be accurately constrained; however, from arrays observed on the open pit walls and intersected in exploration drill holes, these zones appear to be no more than 15–20 m in vertical extent.

Therefore the cross-sectional geometry of the N-dipping individual sigmoid veins arranged en échelon in S-dipping arrays would be consistent with the classical interpretation that only one half of a conjugate pair developed in localized zones of shear ± some dilatation. Why did the conjugate N-dipping arrays not develop in

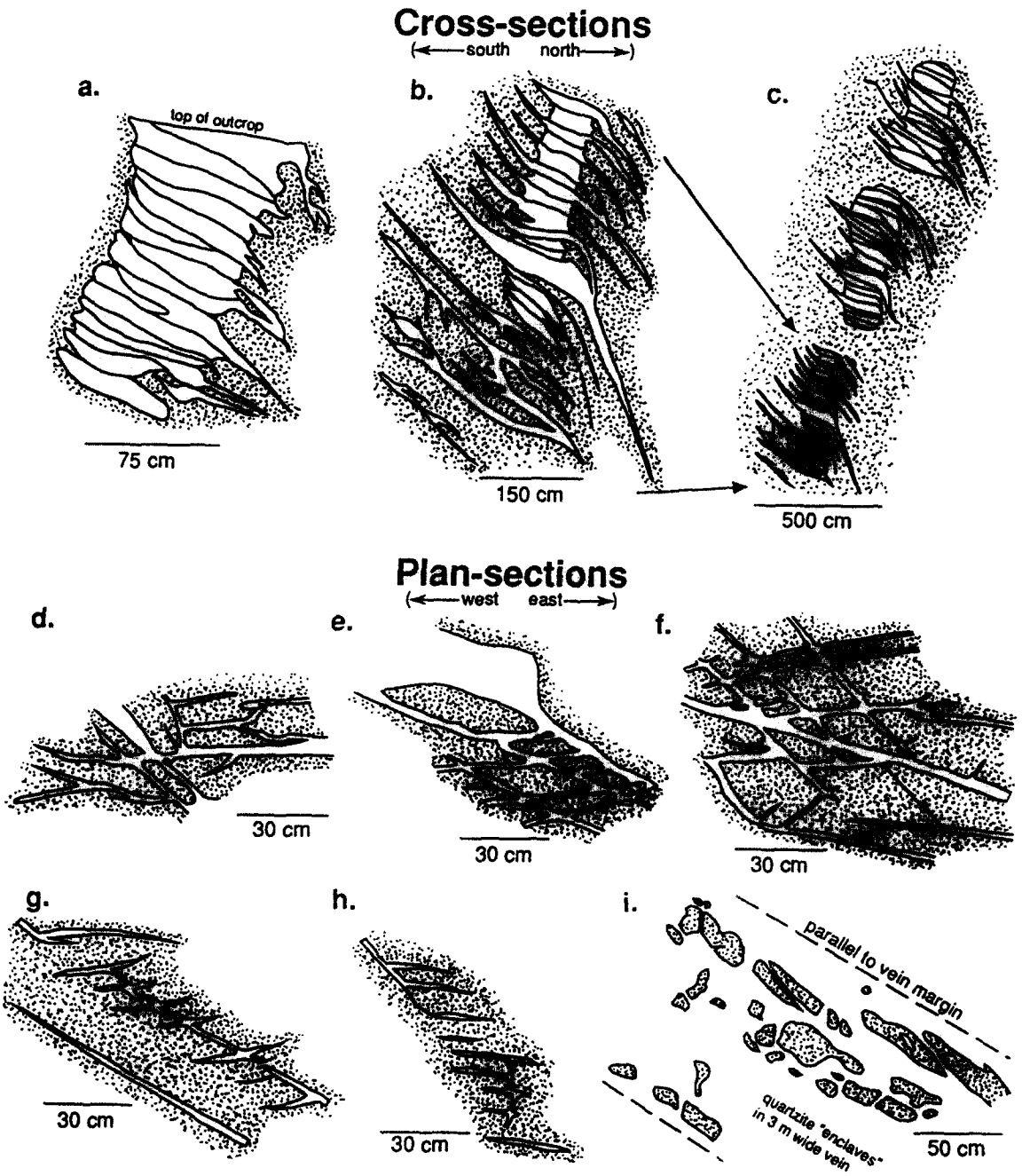

Fig. 4. Field sketches of vein arrays in study area. (a)&(b) North-dipping individual veins are arranged en échelon in S-dipping arrays. (c) Many arrays are themselves arranged en échelon in larger S-dipping zones. (d)–(h) Two sets of mutually cross-cutting veins form rhombohedral and pinnate geometries in plan view of weakly developed arrays. (i) In larger and better developed vein arrays, 'enclaves' of quartzite are aligned parallel to the margins of the arrays.

this vein system? Ramsay & Graham (1970) and Ramsay & Huber (1987) proposed that the unequal development of en échelon arrays in a conjugate pair is due to the progressive rotation of the principal stress directions relative to the rock body during formation of the veins. This rotation results in a bulk noncoaxial deformation. There are two possible explanations why this progressive change in axes' orientations occurred in the White Range. First, the topographic high of the nearly cylindrical orogen was probably to the north of the White Range in the more internal zone of the orogen resulting in an asymmetry in the boundary conditions surrounding the range. Normal sense-of-shear movement along S-dipping arrays would have been favored by the increase in 'free surface' to the foreland of the range and the preferential orogenic collapse in this direction. A second explanation is that minor S-directed movements of the overlying basement thrust sheet would have inhibited dilatation of N-dipping arrays and facilitated dilatation of S-dipping arrays during vein growth. This S-directed movement could have been due to partitioning of displacement along flats (e.g. the basement–quartzite contact at White Range) and ramps during extensional N–S collapse of the orogen or during late residual movement of the contractional thrust system. The late movement along the basement–quartzite contact inhibited the

Fig. 5. Map of vein arrays and a few larger individual veins in one part of White Range mine area (contour intervals in meters; theodolite surveying and compass triangulation were used during mapping of arrays). Vein array traces shown in rose diagram. The larger vein arrays in this map area were mined along S-dipping stopes *ca* 1900–1910.

development of N-dipping vein arrays and resulted in the contemporaneous formation of late minor S-verging folds with E–W-oriented fold hinges.

The classical interpretation for vein arrays and their geometries would predict *one* dominant trace of the veins and arrays in plan view on the horizontal to moderately dipping surface slope of the range given that the intersection between veins and vein array envelopes is approximately horizontal (e.g. Wilson 1961, 1982, Ramsay & Huber 1987). This is not the case. Rather, the traces of individual veins and vein arrays follow *two* dominant trends from the outcrop to the kilometer scale. The strike of over 200 individual veins measured throughout the study area are concentrated about 082° and 118° (Fig. 3c) and the traces of many vein arrays, which were mapped in one portion of the study area (Fig. 5), are similarly concentrated about these two directions (Fig. 3c). In the smaller arrays, individual veins of these two distinct sets commonly intersect to form rhomboids (Figs. 4d–f) and less commonly pinnate geometries (Figs. 4g&h). No consistent cross-cutting relationships were observed between individual veins; ENE-striking veins both displaced and were displaced by ESE-striking veins. It is apparent from the mutually cross-cutting relationship of the veins following these two trends that they formed penecontemporaneously and did not form during two distinct vein-forming events.

This detailed geometry is more difficult to observe in the larger, more fully developed arrays where one set of veins generally dominates the array; rather, the quartzite appears only as enclaves aligned parallel to the array's envelope (Fig. 4i). Both ENE- and ESE-striking arrays are equally well developed (Fig. 5). The arrays do not typically intersect each other, but are spaced meters to tens of meters apart. The horizontal extent of most of these arrays is on the order of 5–15 m, although a few arrays up to 35 m in length are present. All of the observations and data indicate that the arrays trend ENE (strike of 80–90°) and ESE (strike of 110–120°) with moderate dips (50–80°S).

Mapping clearly shows that zones of concentrated veining on the scale of hundreds of meters anastomose around zones of unveined quartzite (Fig. 6). The unveined zones are rhomboids, with their long diagonal trending approximately E–W, and long to short diagonal ratios approximately 2 to 1. This macroscopic anastomosing geometry on the order of hundreds of meters mimics the rhombohedral geometry produced by individual cross-cutting veins on the mesoscopic scale (Figs. 4d–f).

Apart from a few anomalously large vein arrays along the northwestern margin of the study area, the size and frequency of veins and arrays are greatest in the presently exposed center of the vein system and systematically decrease laterally towards the northern, western, and southern margins of the study area. There are no indications of how far east the vein system laterally extends under the basement gneisses of the roof thrust. The vertical extent of the vein system is greatest below the now eroded roof thrust contact at the center of the exposed vein system (based upon drill hole data and open pit exposures). Therefore the vein system is spatially, and probably genetically related to the quartzite–basement contact of the roof thrust. The three-dimensional zone of veining would thus be contained within a concave-upward envelope which is bounded on top by the basement thrust sheet.

STRUCTURAL INTERPRETATION

Three lines of evidence suggest that folding, fracturing and veining are related. First, the folds, fractures and veins are the last structures to overprint the mylonitic fabric of the ductile duplex, and no significant post-Alice Springs Orogeny deformation has been recognized in the region (Wells *et al.* 1970, Shaw *et al.* 1971). In addition, the three structural elements are symmetrically arranged, and there is no clear cross-cutting relationship between those elements. Finally, the gold-

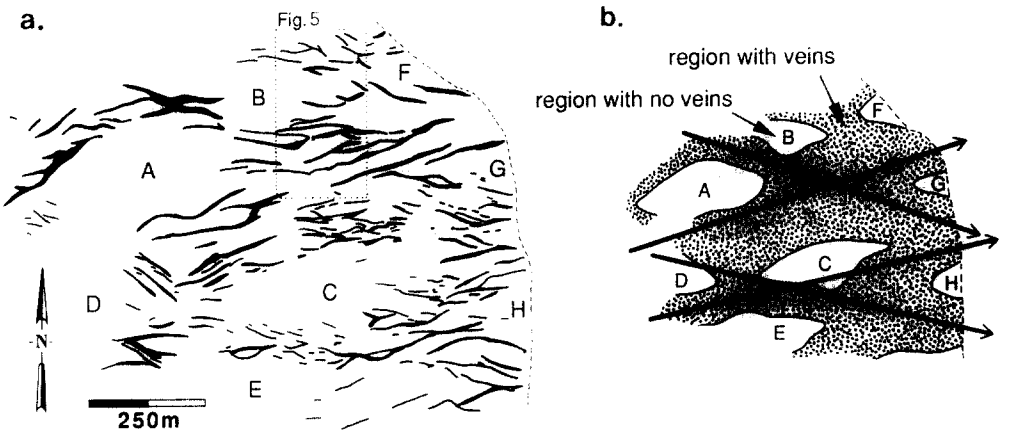

Fig. 6. (a) Generalized large-scale distribution of veins in mine area (map provided by White Range Gold N.L.). Bold lines denote isolated vein arrays or more commonly zones of closely spaced vein arrays (compare with detailed map of Fig. 5). Vein-rich zones anastomose around unveined zones of quartzite (areas A–H). (b) The macroscopic geometry of veined zones grossly mimics the mesoscopic rhombohedral geometry of individual veins (cf. Figs. 4d–f).

bearing vein system of White Range is localized along the broad hinge zone of the large NE-trending antiform.

The following scenario is proposed for the temporal evolution of the vein system. North-over-south thrusting responsible for duplex development virtually ceased during the waning stages of the mid-Paleozoic Alice Springs Orogeny. Orogen subparallel contraction of the nappe complex then produced constrictional fabrics, NE-trending, open, upright folds and kink folds in the White Range (Kirschner & Teyssier 1992). Fracturing and vein formation initiated at the quartzite–basement gneiss contact near the hinge zone of the largest evolving antiform. During folding, the vein system propagated laterally along and vertically downwards from the roof thrust contact. Minor, residual north-over-south shearing prevented N-dipping vein arrays from developing.

In the following discussion, we present the geometric relationships between the fractures, veins, and antiform in order to show that the vein system formed during bulk non-plane-strain deformation resulting in horizontal E–W contraction and N–S horizontal extension. We will then explain the geometry of the veins and arrays in terms of the orthorhombically arranged displacement zone concept.

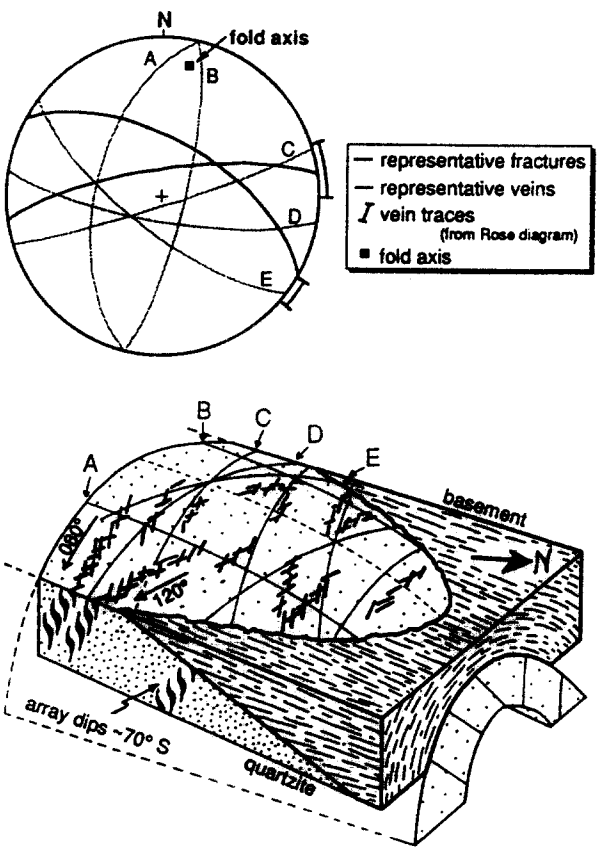

Fig. 7. Representative fold axis, fractures and veins of study area. Fracture sets A–E are symmetrically arranged relative to fold axis. Strikes of individual veins and arrays approximate the strikes of fracture sets C and E, and are bisected by set D. These geometric relations support the hypothesis that a systematic stress–incremental strain field persisted throughout late folding, fracturing and veining, and that vein formation occurred during bulk non-plane-strain deformation.

Symmetry between fractures, fold and veins

The five fracture sets recorded in the orientation data of White Range exhibit three important geometric relationships with the fold axis of the large NE-trending, open, upright antiform (Fig. 7). First, the fold axis 012,17°N lies close to the plane that bisects the two NE-striking fracture sets (sets A and B). Secondly, the same bisecting plane intersects the representative great circles of the other three fracture sets (sets C, D and E) along *one* line 235, 71°S. And finally, fracture set D is within 5° of being orthogonal to the fold axis. The fracture sets are approximately arranged in orthorhombic symmetry to the open upright antiform.

The symmetry between fracture sets and fold elements has been documented by many workers (see reviews by Pollard & Aydin 1988, Hancock 1985), and is generally attributed to: (1) fracturing resulting directly from folding (e.g. Van Hise 1896, Harris *et al.* 1960); and (2) fracturing not resulting from folding, nor necessarily contemporaneous with folding, but occurring in a similarly oriented stress field that produced folding (Price 1966, Engelder 1982a,b). We suggest that this latter scenario applies to the White Range because fractures of similar orientations are also present in the overlying regional thrust sheet and are not directly related with NE-trending folds. Thus the symmetry of the fractures

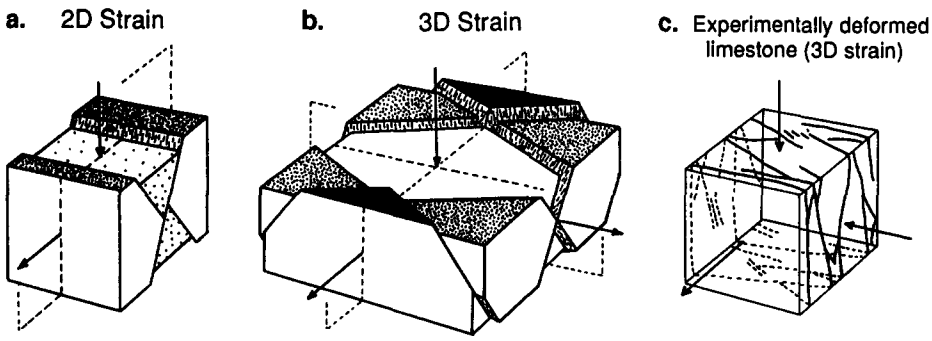

Fig. 8. (a) Conjugate faults develop during bulk coaxial plane-strain deformation. (b) Activation of four sets of penecontemporaneous faults arranged in orthorhombic symmetry results in bulk triaxial strain. (c) Fractures experimentally produced in a limestone cube during bulk triaxial strain by Reches & Dieterich (1983, RD-71 sample inverted).

and NE-trending folds in White Range would suggest that a systematic stress field persisted throughout late open folding and fracturing.

The two distinct sets of veins and arrays exhibit two important structural relationships with the fractures and fold. First, the strike of the two vein sets approximates the strike of fracture sets C and E, and the strike of fracture set D bisects the strike of the two vein sets. Secondly, the strike of the plane perpendicular to the fold axis approximately bisects the strike of the two vein sets. The overall symmetry of the individual veins, vein arrays, fractures and fold is triclinic, though the symmetry is not far from being orthorhombic.

Can the two distinct sets of gold-bearing veins and arrays of White Range be considered a conjugate pair (as proposed by Mackie 1986)? For en échelon vein arrays to be conjugate there must exist a relatively high degree of symmetry between the two sets, unless subsequent deformation has overprinted and modified that symmetry. Four elements are colinear in a conjugate pair of vein arrays (Fig. 1a) (Ramsay & Huber 1987): (1) the fold axis of individual sigmoid veins; (2) the intersection lineation between array envelopes; (3) the intersection lineation between an individual vein and its array envelope; and (4) the intersection lineation between two cross-cutting individual veins. These four linear elements are not colinear for the gold-bearing veins of White Range: the fold axes of sigmoid veins trend approximately E–W, and are subhorizontal; the intersections between array envelopes trend N–S and plunge moderately to the south; the intersections between individual veins and their arrays trend approximately E–W and plunge subhorizontally; the intersections between individual veins are either E–W and subhorizontal or N–S and plunging to the north. Given the non-coincidence of the linear elements, these vein sets cannot be considered as one conjugate pair.

However, the gold-bearing vein sets are unique in mineralogy and geometry on the limb of the antiform, with no consistent cross-cutting relationships to suggest that they formed during distinct events. In addition, the apparent symmetry between the vein sets, fractures sets and antiform suggest that they are geometrically and possibly genetically related. If this is the case, what model can be used to explain their geometry?

Orthorhombic vein array model

We propose a model for en échelon vein arrays in which up to four sets of orthorhombically arranged arrays develop depending upon bulk strain (Fig. 1). In this model conjugate arrays form during bulk coaxial plane strain, while four sets of orthorhombically arranged arrays form during bulk coaxial non-plane strain. During non-coaxial deformations, the number of arrays are reduced to one for plane-strain and two for non-plane-strain deformation.

This model for vein arrays is similar to and the natural extension of the models proposed to explain the orthorhombic patterns of brittle fractures and faults during bulk non-plane-strain deformation (Fig. 8). Oertel (1965) was the first to document the synchronous formation of three to four sets of faults during non-plane-strain deformation experiments involving clay. These sets of faults were arranged in an orthorhombic symmetry such that the three mirror planes of symmetry were coincident with the principal planes of bulk finite strain. He argued that the presently accepted failure criteria were either inappropriate (e.g. Tresca's) or incapable (e.g. Coulomb's) of explaining the geometry and kinematics of the four fault sets unless there were large systematic spatial inhomogeneities in stress and/or strain rate within the deforming clay cake. Discounting this possibility, he formulated a mechanical model which assumes that the mutual interference of slip between faults determines the formation of the fault sets during non-plane-strain deformation.

Following Oertel's work it became apparent from field studies that three or more mutually cross-cutting fault sets have developed contemporaneously in naturally deformed rocks. Aydin (1977) observed four fault sets in sandstone in Utah. Reches (1978a) documented four sets of faults in sandstone in the Palisades monocline of Grand Canyon, Arizona. He suggested that many of the fault patterns observed in the Basin and Range (cf. Donath 1962) could be reinterpreted as forming three or more contemporaneous fault sets (Reches 1978b). In order to account for these fault patterns, Reches (1978b, 1983) provided a mechanical model in which the four active fault sets, in a prefractured rock body, are those that require the lowest stress difference

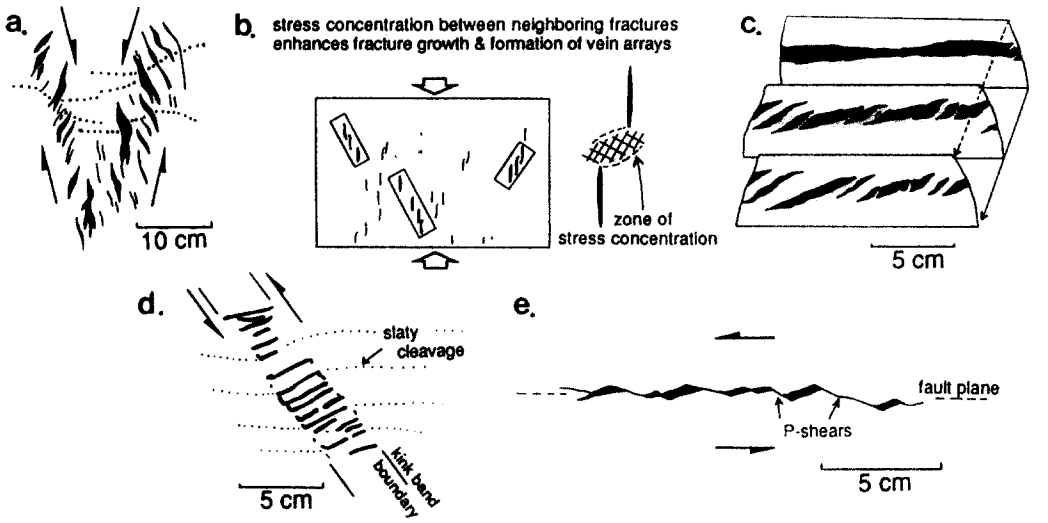

Fig. 9. Five models for the development of vein arrays. (a) Veins formed in zones undergoing shear±dilatation (drawn from fig. 2 of Beach 1975 and fig. 26.15 of Ramsay & Huber 1987). (b) Results of numerical model by Olsen & Pollard (1991), fig. 9a) in which the growth of tensile fractures in en échelon arrays is promoted by the enhanced tensile stresses (or lower compressive stresses) in the overlap region between individual fractures. (c) En échelon veins emanating from a single parent vein as seen in serial sections within a sandstone cobble (drawn from fig. 4 of Nicholson & Ejiofor 1987). (d) Veins formed in dilational zones within a kink band (drawn from plate 2b of Anderson 1968). (e) Veins formed in dilational zones between adjacent P-fractures (drawn from fig. 3 of Gamond 1987).

for slipping and simultaneously minimize the work done by the external forces. Reches & Dieterich (1983) experimentally confirmed in a series of triaxial deformation experiments of sandstone, granite and limestone that the number of faults which develop depends on the imposed bulk strain (Fig. 8c): three or four sets of faults invariably developed during imposed non-plane-strain displacements, and one or two sets formed in response to bulk plane-strain displacements. Krantz (1988, 1989) provided a similar geometric and kinematic model to correlate the arrangement of the multiple fault sets and the relative principal bulk strains. He applied his model to fault patterns in Utah, Nevada, Israel and Crete.

This concept of orthorhombically arranged displacement zones has only been applied to brittle faults. We extend this concept to include brittle–ductile zones of localized displacement. It is most straightforward to extend the concept of orthorhombic displacement zones to vein arrays formed in shear zones (type 'a' in Fig. 9) (Wilson 1952, 1982, Roering 1968, Lajtai 1969, Hancock 1972, type 1 arrays of Beach 1975, Durney 1979, Ramsay 1982), though the concept is applicable to the formation of other vein arrays in which deformation and displacement are localized (e.g. veins contained within kink bands—Anderson 1968, Garnett 1974, Hanmer 1982, Ramsay & Huber 1987; veins contained in dilating shear fractures—Gamond 1983, 1987, Ramsay & Huber 1987). For the type (a) vein arrays in Fig. 9, the en échelon veins form in shear zones where an otherwise ductilely formed fabric is disrupted by the discontinuous vein structures (brittle–ductile shear zones, Ramsay 1980). There is no abrupt transition in the gross geometry and kinematics between zones of localized simple shear which are accommodated entirely by brittle processes (brittle fault zone) and by both brittle and ductile processes (brittle–ductile shear zones); though the geometry and kinematics of brittle–ductile shear zones can be more complex given the involvement of ductile deformation localized within the shear zone. The wall rocks adjacent to brittle–ductile shear zones are much less deformed or even undeformed relative to rocks within the shear zones, thus the brittle–ductile shear zones have localized most, if not all of the deformation and displacement in the rock mass.

The kinematics between brittle fault zones and brittle–ductile shear zones can be similar. A planar brittle fault can only accommodate large displacements parallel to the fault plane. In contrast, a brittle–ductile shear zone can accommodate any imposed displacement within the zone because some of the imposed displacement can be accommodated both by shear parallel to the shear zone boundary and by layer-parallel and -perpendicular extension or contraction by ductile deformation processes (Ramsay & Graham 1970, Simpson & De Paor 1993). Contraction or extension parallel to the planar shear zones will either result in large strain gradients or strain incompatibilities at the shear zone–wall rock contacts because the brittle–ductile shear zone localizes the deformation and the wall rock remains much less deformed, or even undeformed (for similar discussions see Sanderson 1982 for faults and Dewey 1965 for kink bands). Strain compatibility can only be maintained if both the zone and wall rocks homogeneously contract or extend parallel to the planar zones (Ramsay & Graham 1970). Thus, an individual zone or conjugate pair of brittle–ductile shear zones, in an otherwise undeformed rock mass, can only accommodate significant amounts of bulk plane-strain deformation (Fig. 1a). In order to accommodate significant bulk non-plane coaxial strain deformation by brittle–ductile shear zones, we propose that more than two brittle–ductile shear zones must develop with an orthorhombic sym-

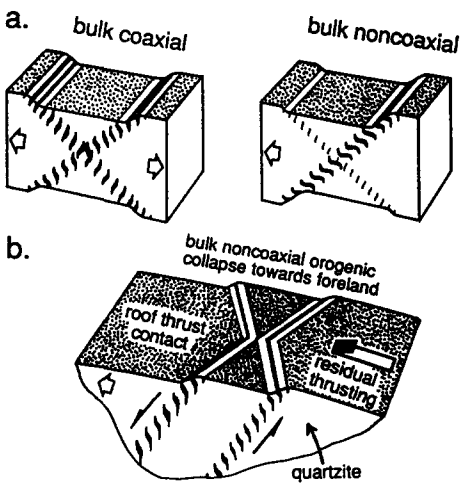

Fig. 10. (a) Relative development of each vein array in a conjugate pair depends, in part, on the coaxiality of deformation (reproduced with minor modifications from Ramsay & Graham 1970). (b) Minor north-over-south movement along the basement–quartzite contact and/or preferential orogenic collapse towards the foreland resulted in bulk non-coaxial deformation which inhibited the development of N-dipping vein arrays in the White Range.

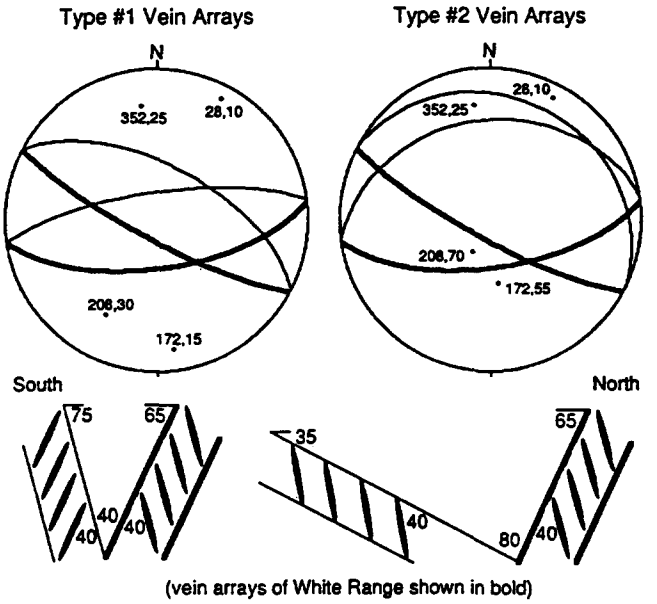

Fig. 11. Two geometric models for orthorhombic arrangement of vein arrays (S-dipping arrays in White Range shown in bold): (1) vein tips are coplanar with the envelope of the associated array (type 1 of Beach 1975); and (2) vein tips in each pair are coplanar (type 2 of Beach 1975).

metry. Four sets of arrays develop during coaxial non-plane-strain deformations (Fig. 1b) and two non-conjugate sets of arrays develop during non-coaxial non-plane strain deformations. The formation of singular and conjugate arrays is restricted to bulk plane-strain deformation.

Application of model to White Range

The vein arrays in the White Range accommodated normal sense-of-shear displacement±horizontal N–S dilatation. This resulted in local vertical shortening and horizontal N–S extension concomitant with orogen sub-parallel shortening and folding. The White Range did not experience bulk plane-strain deformation during vein formation and the two sets of vein arrays do not form one conjugate pair. The two S-dipping sets of arrays formed during bulk non-plane-strain deformation and are one half of four orthorhombic zones. The two sets of N-dipping vein arrays did not develop either due to preferential orogenic collapse to the foreland or non-coaxial deformation resulting from minor residual movement along the overlying basement–quartzite contact (Fig. 10). The orientations for the undeveloped N-dipping arrays can be constrained by utilizing the two end-member geometries commonly observed in vein arrays (Beach 1975) and the 40° angular relationship between vein tips and envelope of the S-dipping en échelon arrays (Fig. 11). If the vein tips in one array were parallel to the envelope of the other array (type 1 geometry of Beach 1975), the N-dipping arrays would dip steeply (60–75°) to the north. If the vein tips in a pair of arrays were all coplanar (type 2 geometry of Beach 1975), the N-dipping arrays would be dipping moderately (20–35°) to the north. The former case (type 1) would most nearly fit an orthorhombic geometry for the whole structural system, including folds and fractures.

Due to the lack of N-dipping vein arrays, the relative bulk displacements responsible for the evolution of the orthorhombically arranged vein arrays cannot be uniquely constrained since the bulk displacement depends on the orientations, magnitudes and directions of shear±dilation of individual arrays, spacing between coplanar arrays and relative activity of the different arrays (cf. Reches 1983, Krantz 1988). Clearly, however, the normal sense-of-shear movement along the S-dipping arrays resulted in extension of subhorizontal N–S-oriented lines. Subhorizontal E–W-trending lines were probably contracting, although the amount of contraction or extension depends on the slip directions and displacements accommodated by the individual arrays (Fig. 11).

CONCLUSIONS

The number and geometry of en échelon vein arrays is dependent on the bulk finite strain imposed on the deforming rock and the degree of coaxiality. The classical interpretation for singular or conjugately arranged arrays is restricted to bulk plane-strain deformations. The degree of coaxiality of deformation determines if only a single set of arrays forms (strongly non-coaxial), or whether two unequally developed (moderately non-coaxial) or two equally well developed sets of conjugate arrays (coaxial deformation) form. Bulk non-plane-strain deformations cannot be accommodated by two conjugately arranged zones, otherwise strain compatibility is not maintained at the contacts between the relatively undeformed host rock and the brittle–ductile shear zones containing the arrays. Four sets of arrays are required to accommodate significant non-plane strain

coaxial deformation, while two non-conjugate sets of arrays can accommodate bulk non-plane non-coaxial deformation. The two contemporaneous sets of vein arrays from the White Range, central Australia, formed during non-coaxial non-plane-strain deformations in the waning stages of the Alice Springs Orogeny.

This model for en échelon vein-array geometries and kinematics is similar to models proposed for brittle faults. The number and geometry of other planar discrete zones in the brittle–ductile realm (e.g. kink bands) which localize deformation and displacement to the near exclusion of any host-rock deformation might also depend on bulk strain and coaxiality of deformation.

Acknowledgements—D. L. Kirschner thanks Ron and Frances James, Jim Cowie, Keith Yates and others of White Range Gold N.L. for their help, hospitality and friendship during his stay at the mine, William Power for a beneficial discussion during the early stage of this work, and Jim Dunlap for discussing field relations. We also thank Jim Dunlap, Adolf Yonkee, John Craddock, John Ramsay and Dorothee Dieterich for their comments on this paper. Support from National Science Foundation grants EAR-8720755 and EAR-9005583 to C. Teyssier and from the Graduate School, University of Minnesota, is gratefully acknowledged.

REFERENCES

Anderson, T. B. 1968. The geometry of natural orthorhombic systems of kink bands. In: *Kink Bands and Brittle Deformation* (edited by Baer, A. J. and Norris, D. K.). *Geol. Surv. Pap. Can.* **68-62**, 200–225.

Aydin, A., 1977. Faulting in Sandstone, Utah. Unpublished Ph.D. thesis, Stanford, California.

Beach, A. 1975. The geometry of en échelon vein arrays. *Tectonophysics* **28**, 245–263.

Collins, W. J. & Teyssier, C. 1989. Crustal scale ductile fault systems in the Arunta Inlier, central Australia. *Tectonophysics* **158**, 49–66.

Dewey, J. F. 1965. Nature and origin of kink bands. *Tectonophysics* **1**, 213–242.

Donath, F. A. 1962. Analysis of basin-range structure, South-central Oregon. *Bull. geol. Soc. Am.* **73**, 1–16.

Dunlap, W. J., Teyssier, C., McDougall, I. & Baldwin, S. 1991. Ages of deformation from K/Ar and $^{40}Ar/^{39}Ar$ dating of white micas. *Geology* **19**, 1213–1216.

Dunlap, W. J. 1992. Structure, kinematics, and cooling history of the Arltunga Nappe Complex, central Australia. Unpublished Ph.D. thesis, University of Minnesota.

Durney, D. W. 1979. Dilation in shear zones and its influence on the development of en échelon fractures. Shear Zone Conference Barcelona, 30–31.

Engelder, T. 1982a. Is there a genetic relationship between selected regional joints and contemporary stress within the lithosphere of North America? *Tectonics* **1**, 161–177.

Engelder, T. 1982b. Reply. *Tectonics* **1**, 465–470.

Forman, D. J. 1971. The Arltunga Nappe Complex, MacDonnell Ranges, N.T., Australia. *J. geol. Soc. Aust.* **18**, 173–182.

Gamond, J. F. 1983. Displacement features associated with fault zones: a comparison between observed examples and experimental models. *J. Struct. Geol.* **5**, 33–45.

Gamond, J. F. 1987. Bridge structures as sense of displacement criteria in brittle fault zones. *J. Struct. Geol.* **9**, 609–620.

Garnett, J. A. 1974. A mechanism for the development of en échelon gashes in kink zones. *Tectonophysics* **23**, 129–138.

Hancock, P. L. 1972. The analysis of en échelon veins. *Geol. Mag.* **109**, 269–276.

Hancock, P. L. 1985. Brittle microtectonics: principles and practice. *J. Struct. Geol.* **7**, 437–457.

Hanmer, S. K. 1982. Vein arrays as kinematic indicators in kinked anisotropic materials. *J. Struct. Geol.* **4**, 151–160.

Harris, J., Taylor, G. L. & Walper, J. L. 1960. Relation of deformational fractures in sedimentary rocks to regional and local structures. *Bull. Am. Ass. Petrol. Geol.* **44**, 1853–1873.

Kirschner, D. L. & Teyssier, C. 1992. Deformation history of the White Range Duplex, central Australia, with implications for fold reorientation. *Aust. J. Earth Sci.* **39**, 441–456.

Krantz, R. W. 1988. Multiple fault sets and three-dimensional strain: theory and application. *J. Struct. Geol.* **10**, 225–237.

Krantz, R. W. 1989. Orthorhombic fault patterns: the odd axis model and slip vector orientations. *Tectonics* **8**, 483–495.

Lajtai, E. 1969. Mechanics of second order faults and tension gashes. *Bull. geol. Soc. Am.* **80**, 2253–2272.

Mackie, A. W. 1986. Geology and mining history of the Arltunga goldfield, 1887–1985. *Northern Territory geol. Surv. Rep.* **2**.

Nicholson, R. & Ejiofor, I. B. 1987. The three-dimensional morphology of arrays of echelon and sigmoidal, mineral-filled fractures: data from north Cornwall. *J. geol. Soc. Lond.* **144**, 79–83.

Oertel, G. 1965. The mechanism of faulting in clay experiments. *Tectonophysics* **2**, 343–393.

Olson, J. E. & Pollard, D. D. 1991. The initiation and growth of en échelon veins. *J. Struct. Geol.* **13**, 595–608.

Price, N. J. 1966. *Fault and Joint Development in Brittle and Semi-brittle Rock*. Pergamon Press, Oxford.

Pollard, D. D. & Aydin, A. 1988. Progress in understanding jointing over the past century. *Bull. geol. Soc. Am.* **100**, 1181–1204.

Ramsay, J. G. 1980. Shear zone geometry: a review. *J. Struct. Geol.* **2**, 83–99.

Ramsay, J. G. 1982. Rock ductility and its influence on the development of tectonic structures in mountain belts. In: *Mountain building processes* (edited by Hsu, K. J.). Academic Press, London, 111–127.

Ramsay, J. G. & Graham, R. H. 1970. Strain variation in shear belts. *Can. J. Earth Sci.* **7**, 786–813.

Ramsay, J. G. & Huber, M. 1987. *The Techniques of Modern Structural Geology, Volume 2: Folds and Fractures*. Academic Press, London.

Reches, Z. 1978a. The development of monoclines. Part I: Structure of the Palisades Creek branch of the East Kaibab monocline, Grand Canyon, Arizona. In: *Laramide Folding Associated with Basement block Faulting in the Western United States* (edited by Matthews, V.). *Mem. geol. Soc. Am.* **151**, 235–272.

Reches, Z. 1978b. Analysis of faulting in three-dimensional strain field. *Tectonophysics* **47**, 109–129.

Reches, Z. 1983. Faulting of rocks in three-dimensional strain fields II. Theoretical analysis. *Tectonophysics* **95**, 133–156.

Reches, Z. & Dieterich, J. 1983. Faulting of rocks in three-dimensional strain fields. I. Failure of rocks in polyaxial, servo-control experiments. *Tectonophysics* **95**, 111–132.

Roering, C. 1968. The geometrical significance of natural en échelon crack-arrays. *Tectonophysics* **5**, 107–123.

Sanderson, D. J. 1982. Models of strain variation in nappes and thrust sheets: a review. *Tectonophysics* **88**, 201–233.

Shaw, R. D., Stewart, A. J., Yar Khan, M. & Funk, J. L. 1971. Progress reports on detailed studies in the Arltunga Nappe Complex, Northern Territory. *Bur. Min. Res., Aust. Rec.* **1971/66**.

Simpson, C. & De Paor, D. 1993. Strain and kinematic analysis in general shear zones. *J. Struct. Geol.* **15**, 1–20.

Stewart, A. J. 1971. Potassium–argon dates from the Arltunga Nappe Complex, Northern Territory. *J. geol. Soc. Aust.* **17**, 205–211.

Van Hise, C. R. 1896. Principles of North American Pre-Cambrian geology. *U.S. geol. Surv. 16th Ann. Rep.*, 581–874.

Wells, A. T., Forman, D. J., Ranford, L. C. & Cook, P. J. 1970. Geology of the Amadeus Basin, central Australia. *Bur. Min. Res., Aust. Bull.* **100**.

Wilson, G. W. 1952. A quartz vein system in the Moine Series near Melness, A'Mhoine, North Sutherland, and its tectonic significance. *Geol. Mag.* **89**, 141–145.

Wilson, G. W. 1961. The tectonic significance of small-scale structures and their importance to the geologist in the field. *Ann. Soc. geol. Belg.* **84**, 424–548.

Wilson, G. W. 1982. *Introduction to Small-scale Geological Structures*. George Allen & Unwin, London.